8th US National Combustion Meeting
Organized by the Western States Section of the Combustion Institute
and hosted by the University of Utah
May 19-22, 2013.

Jet fuels and Fischer-Tropsch fuels: Surrogate definition and chemical kinetic modeling

Krithika Narayanaswamy[1], *Perrine Pepiot*[2], *Heinz Pitsch*[1,3]

[1] *Department of Mechanical Engineering, Stanford University,*

[2] *Sibley School of Mechanical and Aerospace Engineering, Cornell University,*

[3] *Department of Mechanical Engineering, RWTH Aachen University, Aachen*

Using surrogate fuels in lieu of real fuels is an appealing concept for combustion studies. There are two main challenges in such an approach: (i) defining an appropriate surrogate, (ii) designing compact and reliable kinetic models that capture all the specificities of the simpler, but still multi-component surrogates. This task is further complicated by the fairly large nature of the hydrocarbons commonly considered as potential surrogate components, since they typically result in extremely large detailed reaction schemes. This work addresses these challenges in a systematic manner.
Surrogates are proposed for jet fuels (JP-8/Jet-A) and Fischer-Tropsch fuels, composed of *n*-dodecane (to represent normal alkanes), iso-octane (to represent branched alkanes), methylcyclohexane (to represent cyclic-alkanes), and *m*-xylene (to represent aromatics). Following this, a so called "Component Library" approach is invoked to develop a chemical kinetic model for the proposed surrogates. The reaction scheme builds upon our recent chemical kinetic modeling efforts, whereby a single chemical mechanism has been developed that has the capability to describe the oxidation of several small hydrocarbons, including *n*-heptane and iso-octane [Blanquart *et al.*, Combust. Flame 2009], moderate to high temperature oxidation of a number of substituted aromatics, including *m*-xylene [Narayanaswamy *et al.*, Combust. Flame (2010)], and low through high temperature oxidation of *n*-dodecane [Narayanaswamy *et al.*, in preparation]. The present work extends this chemical kinetic model to now describe the low through high temperature oxidation of methylcyclohexane. In order to better describe the kinetics of methylcyclohexane oxidation, a few changes have been introduced in the reaction mechanism based on rate recommendations from theoretical and experimental work available in the literature. Extensive validation of the resulting kinetic model is performed for methylcyclohexane using a wide range of experimental data sets. Thereafter, the capabilities of the proposed surrogates and their reaction mechanism are appraised by comparing the model predictions against ignition delay and flame speed measurements for jet fuels and Fischer-Tropsch fuels.

1 Introduction

Transportation fuels are mixtures of several hundreds of compounds belonging to different hydrocarbon classes. Their composition can vary significantly, and only average fuel properties are known at best. The complexity of the real fuels makes it infeasible to simulate their combustion characteristics directly, requiring a simplified fuel representation to circumvent this difficulty. Typically, the real fuels are modeled using a representative surrogate mixture, *i.e.* a well-defined mixture comprised of a few components chosen to mimic some of the physical and chemical properties of the real fuel under consideration.

Guidelines have been developed by different surrogate working groups [1–3] to determine the most relevant components for engine fuel surrogate mixtures, including jet fuels. Several groups

have proposed surrogates involving two, three, or more components for jet fuels and Fischer-Tropsch fuels [4–10]. In this work, we formalize the surrogate definition procedure by adopting an constrained optimization approach, which helps determining the surrogate compositions in order to best represent the target real fuel properties. An interesting related work for diesel fuel surrogates comes from Androulakis et al. [11].

Once the surrogate composition is chosen, compact and reliable kinetic models that capture all the specificities of the simpler, but still multi-component surrogate need to be developed. Several chemical models have been proposed for jet fuel and Fischer-Tropsch fuel surrogates [3, 5, 8, 10, 12–15], but very few are applicable to low as well as high temperatures, while being well-validated and compact enough for practical use. Our objective is to develop such a chemical model that can describe the kinetics of the surrogate accurately at low through high temperatures as well as be amenable to numerical calculations. The kinetic model needs to be well-validated for the individual components of the surrogate fuel, in order to make reliable predictions about the combustion characteristics of the surrogate mixtures. Though detailed mechanisms for many fuel components have been developed, these typically comprise of several thousand species and reactions, for even single component mechanisms. The chemical mechanisms from different sources typically represent similar reaction pathways differently, due to the uncertainty in the kinetic rate data, rendering the combination of these detailed mechanisms to create multi-component mechanisms nearly impossible. Moreover, it is important to maintain consistency in formulating such multi-component mechanisms with respect to how the kinetic rates for the different reaction classes are treated.

In this work, these challenges are addressed in a systematic fashion. The article begins with the surrogate definition in section 2. This is followed by the discussion on the general methodology to develop chemical mechanisms for surrogate fuels, and a demonstration of the approach as applicable to jet fuels (JP-8/Jet-A) and Fischer-Tropsch fuels in section 3. Thereafter, the performance of the proposed surrogates and their reaction mechanism are evaluated by comparing the model predictions against ignition delay and flame speed measurements for JP-8 fuels and for Fischer-Tropsch fuels.

2 Definition of surrogates for JP-8 fuels and Fischer-Tropsch fuels

2.1 Choice of individual components

A natural procedure to select suitable components of the surrogate mixture for a particular fuel, is to identify one representative hydrocarbon, for each of the major hydrocarbon classes found in the real fuel. It is important to choose representative components that have been carefully studied, in order to assess the ability of the surrogate kinetic model for the individual component description, which is in itself key to the performance of the multi-component surrogate model. The major hydrocarbon classes present in a typical JP-8/Jet-A fuel are depicted in Fig. 1(a), namely paraffins, naphthenes and aromatics [4]. In contrast, the Fischer-Tropsch (F-T) fuels are mainly comprised of normal alkanes, branched alkanes and cyclic alkanes [10]. As a direct consequence, the sooting tendencies of F-T fuels are far smaller than the jet fuels, due to the minor amount of aromatics in F-T fuels.

Based on molecules identified as relevant to jet fuels [3], the components of the JP-8 surrogate for

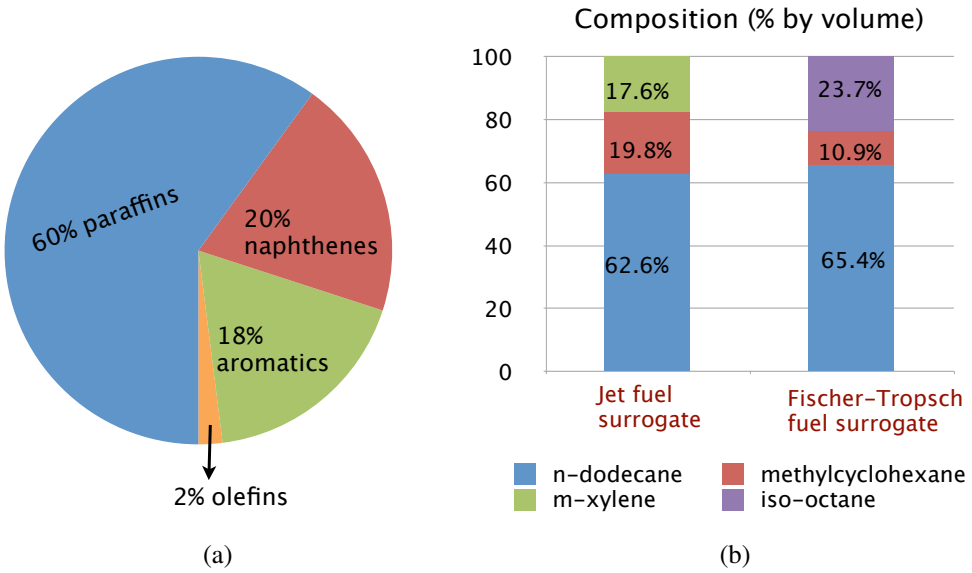

Figure 1: (a) Major hydrocarbon classes found in a typical jet fuel (JP-8/Jet-A) [4] (b) Jet fuel and Fischer-Tropsch fuel surrogates proposed in the present work.

this work have been chosen as: (a) *n*-dodecane, to represent the paraffin class; (b) methylcyclohexane, to represent the naphthene class; and (c) *m*-xylene to represent the aromatics. Similarly, the components of the F-T fuel surrogate have been chosen as *n*-dodecane, methylcyclohexane, and iso-octane, to represent the normal alkanes, cyclic alkanes, and branched alkanes in F-T fuels, respectively. This choice is motivated by several observations. First, *n*-dodecane has physical properties close to JP-8/Jet-A over temperature ranges of 100–650°C [4, 16]. Second, the aromatic component *m*-xylene possessing a higher tendency to soot compared to the other chosen components, helps the surrogate in reproducing the sooting characteristics of the jet fuel. Finally, methylcyclohexane and iso-octane are the simplest substituted cyclic alkane and branched alkane respectively that can be modeled reliably. The global ignition and flame propagation characteristics of these components have been examined in several experimental studies, and some of their key chemical reaction pathways have also been the object of theoretical and experimental kinetic rate determinations. Therefore, having chosen well studied components for the surrogate, extensive validation can be performed for the individual components of the proposed surrogates.

2.2 Composition of individual components

The average properties of typical transportation fuels that are crucial to design a surrogate for combustion applications include the fuel heating value, average carbon number and molecular weight, and the sooting tendencies. The sooting tendency of a hydrocarbon is experimentally determined by measuring the smoke height H, which is the height such that any increase in the fuel flow rate of that hydrocarbon's jet flames would cause them to emit soot. Smoke heights measured in a specific apparatus are converted into apparatus-independent *threshold sooting indices* (TSIs)

Parameters	Gasoline	Jet fuel	Diesel fuel	Fischer-Tropsch fuel
Lower HV (MJ/kg)	43.4	43.3	42.7	44.2
Carbon number range	4–12	8–16	9–23	–
Average formula	$C_{6.9}H_{13.5}$	$C_{11}H_{21}$	$C_{16}H_{28}$	–
Liquid density (kg/l)	0.735	0.775–0.840	0.850	0.736
Molecular weight (g/mol)	~ 96.3	~ 153	~ 220	–
Threshold Sooting Index	–	~ 15 (≤ 40)	–	–
Cetane Number	–	~ 42	40–55	61

Table 1: Average properties of transportation fuels key to define surrogates for combustion applications. Data compiled from several sources [4, 17–19].

using,

$$\mathrm{TSI} = \mathrm{a} \times \frac{\mathrm{MW}}{\mathrm{H}} + \mathrm{b}, \tag{1}$$

where MW is the molecular weight of the hydrocarbon and a and b are apparatus-specific constants chosen so that $\mathrm{TSI}_{\mathrm{ethane}} = 0$ and $\mathrm{TSI}_{\mathrm{naphthalene}} = 100$ [20]. The threshold sooting index has been found to correlate well with actual particulate emissions [21].

The values of these target properties for a few transportation fuels are shown in Table 1. Given a choice of components to make up the surrogate, it is desired to determine an optimized component composition, so that the properties of the surrogate fuel resemble the target real fuel properties. In the present work, this objective is formulated as a constrained optimization problem. The composition of surrogate components are the optimization variables, and average real fuel target properties are the desired optimization targets. The most important targets are imposed through the introduction of constraints in the optimization problem. The constrained optimization approach could in principle be employed to define a surrogate for any real fuel whose relevant target properties are known.

In order to perform the optimization, quantitative structure/property relationships must be available, relating the target real fuel properties to the fuel structure of the individual surrogate components and their mole fractions. In this work, mixture properties are determined by exploiting the fact that most of these target real fuel properties are indeed bulk properties; the multi-component surrogate fuel's properties are hence expressed as combinations of individual component properties, weighted by mole fractions or volume fractions appropriately. Structural group analysis is also used wherever applicable, for instance to determine threshold sooting index of the surrogate fuel. This procedure follows that described by Yan *et al.* [22], based on the initial work of Benson [23].

The optimal component composition of a JP-8 surrogate that is obtained by solving the constrained optimization problem for *n*-dodecane, methylcyclohexane, and *m*-xylene is provided in Table 2, where the target properties used are also listed. The composition of aromatics is primarily determined by the Threshold Sooting Index requirement for the surrogate. By a similar procedure, a surrogate for Fischer-Tropsch fuel could also be proposed using *n*-dodecane, methylcyclohexane, and iso-octane as components as shown in Table 3. The compositions of the proposed surrogates are summarized in Fig. 1(b).

Target properties	Jet-A/JP-8 properties	JP-8 Surrogate
H/C ratio	1.91 ± 0.05	1.94
Average formula	$C_{11}H_{21}$	$C_{9.64}H_{18.75}$
Liquid density (kg/l)	0.810	0.769
Molecular weight (g/mol)	153	134.80
Threshold Sooting Index (TSI)	15	15.34
Composition (% volume)	$\sim 60\%$ paraffins	62% *n*-dodecane
	$\sim 20\%$ cyclo paraffins	19.8% methylcyclohexane
	$\sim 18\%$ aromatics	17.6% *m*-xylene

Table 2: A JP-8 surrogate proposed using the constrained optimization approach.

Target properties	F-T properties	F-T Fuel Surrogate
H/C ratio	2.17 ± 0.05	2.16
Cetane Number	61	60.99
Liquid density (kg/l)	0.736	0.734
Molecular weight (g/mol)	–	142.7
Threshold Sooting Index	–	5.02
Composition (% volume)	normal alkanes	65.4% *n*-dodecane
	branched alkanes	23.7% iso-octane
	cyclic alkanes	10.9% methylcyclohexane

Table 3: A Fischer-Tropsch fuel surrogate proposed using the constrained optimization approach.

From Table 2 it can be seen that the proposed jet fuel surrogate agrees with the target real fuel properties as far as the composition of major hydrocarbons and H/C ratio (which is indicative of the heating value of the jet fuel) is concerned. Also, the Fischer-Tropsch fuel surrogate in Table 3 captures the target properties of the F-T fuel, namely, H/C ratio, liquid density, and cetane number. The sooting tendency of the jet fuel, as measured by the Threshold Sooting Index is also captured by the proposed surrogate. However, discrepancies can be observed for the average chemical formula and the fuel molecular weight comparing the real JP-8 fuel and the proposed surrogate. Using a heavier cyclic alkane in place of methylcyclohexane in the surrogate mixture could help achieve these targets better. In spite of these differences, it will be shown in the later sections that the surrogates proposed here accurately describe the combustion characteristics of the real fuels at high temperatures. Note that the cetane number is not considered as one of the targets in the jet fuel surrogate definition here. It was found that the composition of the different hydrocarbon classes of the jet fuel surrogate would not be similar to that of the real fuel with the current choice of surrogate fuel components if the cetane number constraint were to be included in the surrogate definition. This point will be revisited in the later part of this work in section 4.1.

3 Reaction scheme for the jet fuel and F-T fuel surrogates

At this point, we have a reasonable surrogate composition that can be used in numerical studies in order to identify its strengths and weaknesses and further refine the composition. In this section,

we elaborate on the development of a single, consistent, and reliable chemical scheme to accurately model such surrogate mixtures. The principal idea is based on the so called Component Library approach proposed by Pepiot [24] to construct chemical models for surrogate fuels. This approach is explained first in general here, as applicable to any surrogate mixture. Thereafter, the idea is applied to develop a single, compact chemical model for the jet fuel and Fischer-Tropsch fuel surrogates proposed in section 2.

3.1 Component Library approach

Since the detailed models even of single components are often of a large size, putting together several of these to form the model for a surrogate is clearly not a trivial task. Combining different mechanisms has the risk of introducing truncated paths or involuntarily duplicating reaction pathways. Moreover, practical CFD simulations demand for chemistry models to be as short as possible. We propose here a methodology to construct reduced kinetic models for surrogate fuels that is based on two principles:

- Simplification: Reduction should be done on single component mechanisms, as it reduces both the size of the initial scheme and the extent of the validation domain. Thereafter, these skeletal level models could be combined to come up with mechanisms that can handle mixtures.
- Flexibility: The addition of another component in the definition of the surrogate mixture should not require the entire process to be repeated. Instead, only the parts relevant to this extra molecule should be added. In the same way, if some additional feature, such as the ability to predict nitrogen oxides, is desired, it should be possible to add it without changing the core of the remaining mechanism.

In short, the reduced chemical model for surrogate mixtures is developed as follows. The existing detailed mechanisms for individual components of the surrogate are reduced for various conditions to the skeletal level using two reduction techniques: the DRGEP method [25], and a chemical lumping technique [26]. The collection of skeletal mechanisms forms the so called *component library*, to which several specific modules can be added, such as a description of soot formation or NO_x chemistry. The surrogate composition and its future use dictates the choice of modules that have to be included in the combined skeletal mechanism, so that only the necessary kinetics are taken into account. Then, a second stage of reduction could be applied, that includes for example the introduction of quasi-steady state assumptions.

The obtained reduced model can be analyzed and validated using available experimental data easily owing to its reduced and reasonable size. The analysis of the predictions obtained using the resulting kinetic scheme and the surrogate composition will provide additional constraints to be included in the surrogate definition phase, and the whole process can be repeated until an optimal surrogate is obtained. The major reduction steps, that is DRGEP and lumping, are done only once to obtain the component skeletal mechanism, which minimizes the total time to develop the surrogate mechanism.

3.1.1 *Assumptions and Challenges*

The component library approach as described above and its efficiency are based on two major assumptions. The first one is that two different large hydrocarbon molecules interact during combustion only at the level of small radicals and decomposition products that are present already in both detailed mechanisms. Direct cross-reactions between fuel-specific molecules are neglected. The main argument to justify this assumption involves steric factors: unless the pressure is very high, the reactive sites of large molecules or radicals are much less accessible by another large species than a small radical such as OH. In case the cross-reactions between two compounds are shown to be important, incremental sets containing the relevant reactions could be added in the library.

The second assumption is that not all reaction pathways are important for all configurations. This assumption allows the creation of modules through the reduction of the detailed mechanisms on complementary sub-domains of the parameter space. Then smaller multi-component mixtures are obtained by combining only the modules relevant to the application. The best example of this segregated approach is the temperature dependence of the hydrocarbon oxidation chemistry, which is separated into a high temperature base chemistry and a low temperature module that can be added to this base chemistry to represent the low temperature phenomena.

3.2 Application to the proposed JP-8/Jet-A fuel and Fischer-Tropsch fuel surrogates

The component library approach to arrive at a compact reaction scheme for the proposed jet fuel surrogate is pictorially represented in Fig. 2. This chart describes the assembly of reaction pathways for the individual components of the jet fuel surrogate. The chemical model has been assembled in stages, starting with a base model and adding to it sub-mechanisms for the individual components of the surrogate, namely *m*-xylene, *n*-dodecane, and methylcyclohexane. The chemical model is validated comprehensively every time the oxidation pathways of a new component are incorporated into it. A similar chart could be drawn for the chemical kinetic model development for the proposed Fischer-Tropsch fuel surrogate.

3.2.1 Base model and extension to aromatics

The present work uses the detailed mechanism developed by Blanquart *et al.* [27] as the base chemical model. This mechanism has been developed for the oxidation of thirteen fuels ranging from C_1–C_8 species, and including alkanes such as *n*-heptane and iso-octane, and aromatics species such as benzene and toluene. This kinetic model has been extensively validated against ignition delay times and laminar burning velocities over a wide range of temperatures and pressures, and has also been tested in laminar premixed and diffusion flame configurations.

Subsequently, the reaction pathways to describe the moderate to high temperature oxidation of several substituted aromatics, including *m*-xylene (which is the aromatics class representative in the proposed jet fuel surrogate) were incorporated into the model in a consistent manner [28]. The test cases at high temperatures used for model validation include ignition delays of the substituted aromatics and species time histories data from shock-tube experiments, concentration profiles in

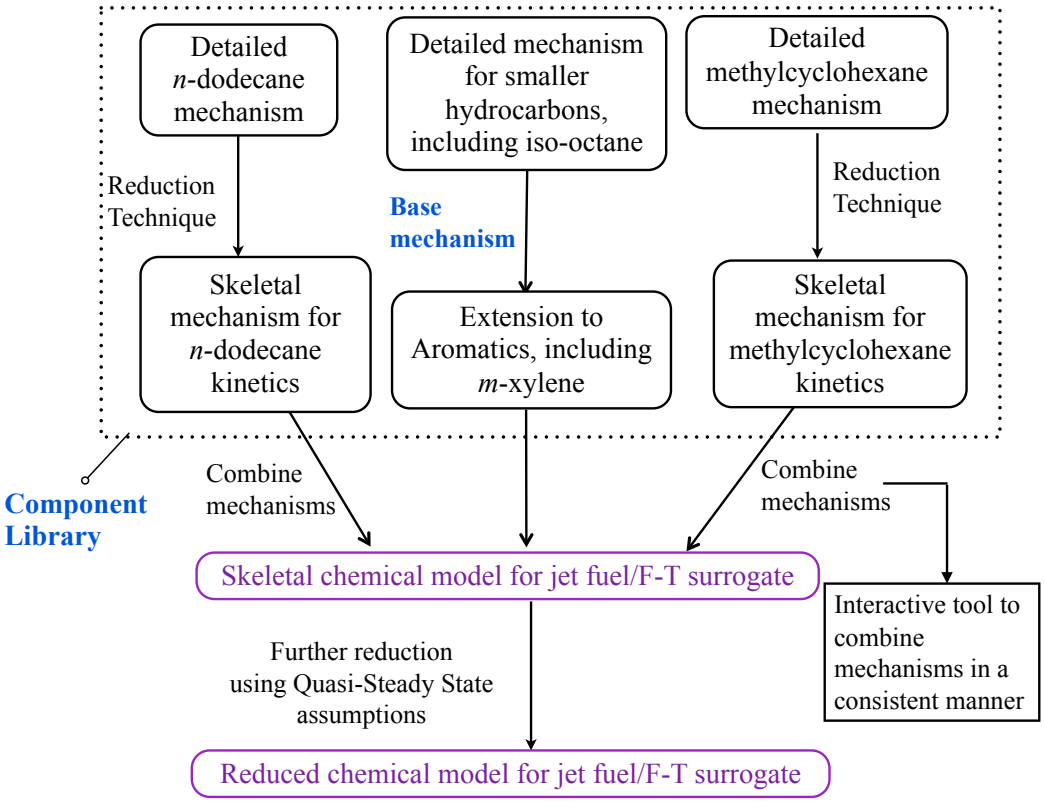

Figure 2: Component Library approach as applicable to the development of a chemical model for the oxidation of the proposed jet fuel surrogate.

plug flow reactors and flame speeds in premixed flame configuration. This discussion will be skipped here for brevity, and the readers are referred to the original article for the validation test results for oxidation of substituted aromatics.

3.2.2 Extension to *n*-dodecane

Recently, the previous reaction scheme that includes the aromatic chemistry [28] was extended to include the reaction pathways of low through high temperature oxidation of *n*-dodecane. A short skeletal level model was obtained from the detailed reaction scheme of Sarathy *et al.* [29] for normal and methyl alkanes using a multi-stage reduction strategy, involving species and reaction elimination using the DRGEP approach [25] and chemical species lumping [26], and integrated into the previous model. A few reaction rate updates were introduced to improve the ignition delay and species profile predictions of the resulting combined model, based on rate recommendations from theoretical and experimental studies in the literature. In addition, the H_2/O_2 chemistry of the combined model was also updated according to the latest Hong *et al.* model [30].

The revised model has been thoroughly validated for *n*-dodecane at lower temperatures for ignition and species concentration profiles, in addition to validation cases at high temperatures, that included ignition delays, species time histories, oxidation and pyrolysis in shock tubes and laminar flame speeds in premixed flames. Similarity among normal alkanes towards ignition behavior and

speed of premixed flame propagation was exploited to investigate the performance of the model. The revised model has demonstrated the capability to predict these validation tests satisfactorily, and will be available in greater detail in our upcoming work [31].

3.2.3 Extension to methylcyclohexane

In order to complete the description of all the components in the proposed surrogates, the next step involves adding a sub-mechanism for the low through high temperature oxidation of methylcyclohexane to the model obtained from the previous sub-section 3.2.2, that includes smaller hydrocarbons, aromatics, and *n*-dodecane. The procedures to extend the chemical model to include kinetics of *n*-dodecane and methylcyclohexane are similar as can be understood from the schematic in Fig. 2, only differing with respect to the reference detailed model, the reduction targets, and the revisions in the kinetic rates subsequently introduced for model improvement.

Several detailed chemical mechanisms have been proposed for methylcyclohexane [8, 12, 32–34]. However, these are detailed/semi-detailed mechanisms, and only few are relevant for low through high temperature oxidation of methylcyclohexane. Further, the relevance of methylcyclohexane as a component of jet fuel surrogates has recently attracted a number of experimental studies, thus widening the experimental database on methylcyclohexane oxidation [35–39]. A majority of these experimental data were obtained after the development of the above mentioned models, and in some cases, those models were not validated against all existing data, for example, species profile measurements. There is therefore a rich experimental database that has yet to be fully utilized for model evaluation and improvement, which will be leveraged in this work.

Of specific interest here is the chemical scheme proposed by Pitz *et al.* [34], where the low temperature reaction pathways for methylcyclohexane oxidation have been added to the high temperature mechanism previously developed by Orme *et al.* [33]. This chemical scheme was validated against ignition delay time data from rapid compression machine studies. The Pitz model has been used as the starting detailed mechanism for methylcyclohexane in the present effort. The methodology associated with the extension to methycyclohexane is discussed next, followed by a summary of the revisions introduced to the model, and validation of the revised model.

Mechanism development

The reference mechanism for methylcyclohexane oxidation from Pitz *et al.* [34] has 8807 forward and reverse reactions among 999 species. This detailed mechanism is first reduced to a skeletal level using a multi-stage reduction strategy, involving species and reaction elimination using the DRGEP approach [25], and chemical species lumping [26]. The database used to carry out the reduction includes plug flow reactor-like configurations, and ignition delays for low to high temperatures (600–1500 K), pressures ranging 1–40 atm, and equivalence ratios spanning lean to rich conditions (0.5–1.5).

The resulting skeletal mechanism for methylcyclohexane consists of 986 reactions and 249 species. In Fig. 3, ignition delays computed using the detailed and skeletal schemes are compared for lean and stoichiometric methylcyclohexane/air mixtures. The comparisons show very good agreement over the entire temperature ranges and at different pressures. A high reduction ratio is achieved

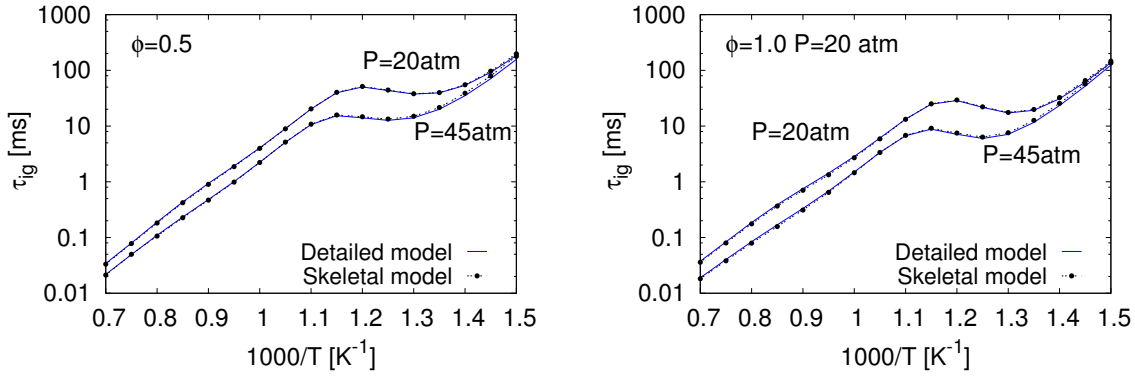

Figure 3: Ignition delay times of methylcyclohexane/air, comparing the skeletal level mechanism with the detailed mechanism results; solid lines - detailed mechanism: Pitz e*t al.* [34].

($\sim$ 75%) and negligible error has been introduced in the skeletal scheme relative to the detailed chemical mechanism. This skeletal scheme is used in the subsequent mechanism development steps.

The merging of the skeletal methylcyclohexane with the previous mechanism (including aromatics and *n*-dodecane) is accomplished using an interactive tool [24] that automatically identifies common species and reactions from the different mechanisms, and incompatibilities between the kinetic data sets. The resulting combined mechanism includes the oxidation pathways of methylcyclohexane at low through high temperatures in addition to several hydrocarbons already described in the previous mechanism. The incremental methylcyclohexane module consists of 471 reactions among 145 species, out of the total 399 species and 2791 reactions (counted forward and backward separately) for the full surrogate reaction mechanism. A sketch of the main oxidation pathways of the fuel (methylcyclohexane) and the ring opening of methylcyclohexyl radicals is shown in Fig. 4(a). The low temperature reaction pathways for one of the methylcyclohexyl radicals retained in this incremental reaction set are provided in Fig. 4(b). In order to ensure a smooth and consistent merging, rate conflicts detected during the merging were always resolved in favor of the thoroughly validated base model, therefore leaving this mechanism virtually unchanged. Further, duplicate reaction pathways in the combined model coming from the incremental methylcyclohexane reaction scheme were identified and removed appropriately.

Need for an improved model

The ignition delays computed using the resulting combined mechanism are compared against data from the shock tube experiments of Vasu *et al.* [40] at $\phi = 1.0$ and $P = 20$ atm in Fig. 5(a). Also plotted in the figure are the ignition delays at low temperatures measured in Rapid Compression Machines (RCM) by Pitz *et al.* [34]. The ignition delay predictions of the combined model are closer to the experimental ignition delay data at high temperatures compared to the skeletal model, while longer than the skeletal model in the *Negative Temperature Coefficient* (NTC) regime, due to the differences in the C_1–C_4 base chemistry. From Fig. 5(a), it can be noted that both these models predict ignition delays which are longer by an order of magnitude compared to the experimental data at all temperatures.

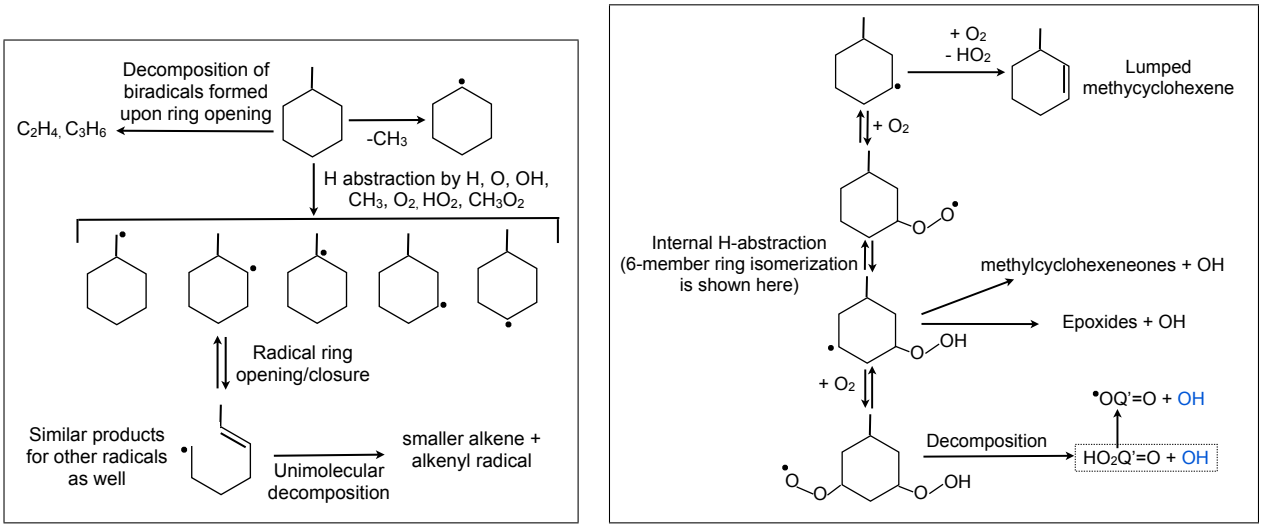

(a) Fuel and radical decomposition pathways (b) Pathways for low temperature chemistry

Figure 4: (a) Main oxidation pathways of methylcyclohexane and the ring opening of methylcyclohexyl radicals (b) Low temperature reaction pathways for one of the methylcyclohexyl radicals retained in this incremental reaction set.

Further, comparing the combined model predictions for OH time histories against shock tube measurements in Fig. 5(b), it can be observed that in contrast to the experimental data, the rise of OH profiles occur later, and without any noticeable peak. These observations certainly suggest that improvements are needed to the combined model predictions. In order to better describe the kinetics of methylcyclohexane oxidation, a few changes have been introduced in the combined mechanism based on rate recommendations from theoretical and experimental work available in the literature. These are motivated by sensitivity analysis studies performed with the combined mechanism, which is facilitated owing to the reasonable size of the reaction scheme.

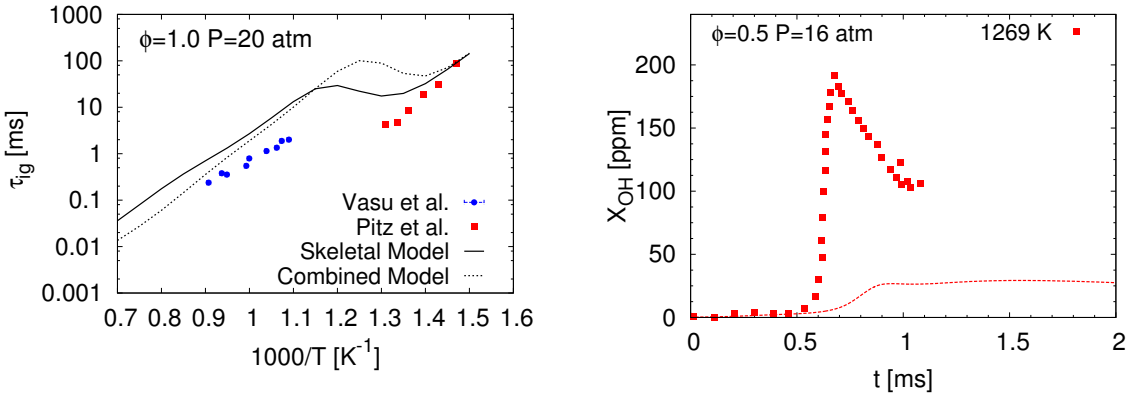

Figure 5: (a) Ignition delay time comparison - experimental data: Vasu e*t al.* [40], Pitz e*t al.* [34]; solid lines: predictions using the skeletal model (b) Comparison of OH time histories - experimental data: Vasu e*t al.* [41]. Dashed lines: predictions using the combined model

Ignition delays at high temperatures show better agreement with the experimental data by a revised treatment of butyl and pentyl bi-radical pathways as suggested by Silke *et al.* [42]. In order to

Shock tubes		Plug Flow Reactor	Burning velocity
Ignition delays	Species profiles		
Vanderover *et al.* [46] Vasu *et al.* [40] Pitz *et al.* [34] Hong *et al.* [35]	Vasu *et al.* [41] Hong *et al.* [35]	Zeppieri *et al.* [47]	Kumar *et al.* [36] Singh *et al.* [37] Ji *et al.* [38] Kelley *et al.* [39]

Table 4: Validation cases for methylcyclohexane undertaken in the present study.

improve the ignition delay predictions in the NTC ignition regime, updates were made to the rates of the most sensitive reactions: (i) ring opening of methylcyclohexyl radicals (see Fig. 4(a)), (ii) reactions involving isomerization of peroxy radicals to hydroperoxy radicals, and (iii) formation reactions of epoxides (cyclic ether) and OH from the hydroperoxy radical as shown in Fig. 4(b), based on recent theoretical studies [43, 44] for their cyclohexyl counterparts. This updated model is validated in the following sub-section.

Validation tests for methylcyclohexane

The test cases considered for methylcyclohexane validation include ignition delay measurements in shock tubes and rapid compression machines. These experiments consider a wide range of temperatures, pressures, and fuel/air mixture ratios. Additionally, validation is performed using OH time histories from shock tube measurements, and laminar flame speed measurements at various pressures. The list of the validation tests, which are discussed in further detail below, appears in Table 4.

Ignition delays are computed using a constant volume homogeneous reactor configuration, using the same ignition criterion as in the experiments. Laminar flame speeds have been calculated in a manner similar to that described in our previous works [27, 28]. All numerical calculations have been performed using FlameMaster version 3.3.9 [45].

Methylcyclohexane/air ignition delays: The ignition delay predictions of the present model are compared against experimental ignition delay time data from the shock tube experiments of Vasu *et al.* [40] at $\phi = 1.0$ and $P = 20$ and 45 atm. In addition, comparisons are performed with the data of Vanderover and Oehlschlaeger [46] at $\phi = 0.25, 0.5$ and 1.0, and $P = 12$ and 50 atm. Also shown in these figures are comparisons against ignition delay times measured in a Rapid Compression Machine by Pitz *et al.* [34] at $\phi = 1.0$, with $P = 15$, 20 atm. The present scheme captures the pressure dependence of the ignition delays as well as the variation with fuel mixture ratios with good accuracy. The computed ignition delays at $900 < T < 1100\,\mathrm{K}$ at $P = 20$ atm appear to be longer than the experimental data, while these show better agreement with data in this temperature range at higher pressures $P = 45$ atm in Fig. 6(b).

The rate changes associated with the cyclic ring opening and closing reactions (see Fig. 4(a)) contribute significantly to shorten the ignition delays in the NTC region and at low temperatures compared to the combined model predictions shown in Fig. 5(a), and are also responsible for the flatter slope $\frac{d\tau_{ign}}{dT}$ in the NTC ignition regime. Accompanied by the other reaction rate updates introduced to the model involving peroxy radical isomerization, and epoxide + OH formation from

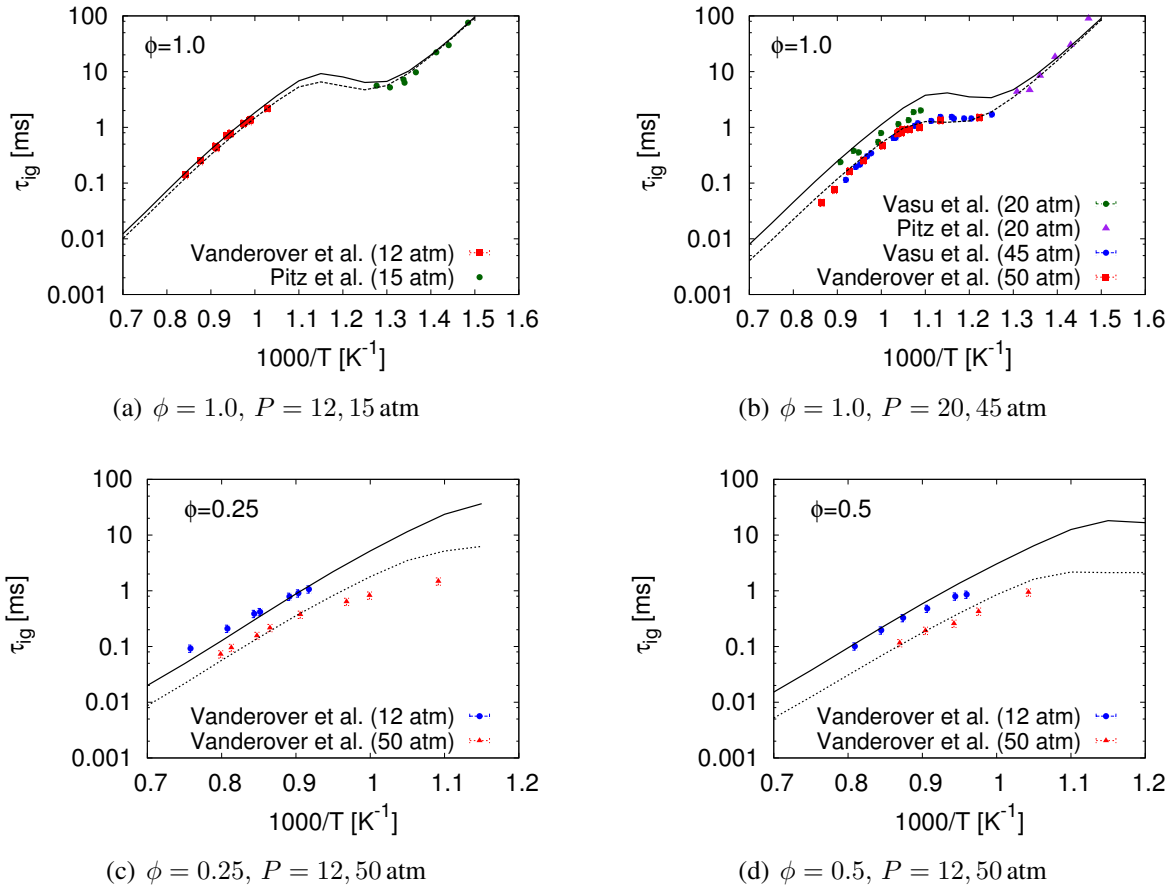

(a) $\phi = 1.0,\ P = 12, 15\,\text{atm}$ (b) $\phi = 1.0,\ P = 20, 45\,\text{atm}$

(c) $\phi = 0.25,\ P = 12, 50\,\text{atm}$ (d) $\phi = 0.5,\ P = 12, 50\,\text{atm}$

Figure 6: Ignition delay times of methylcyclohexane/air mixtures: Symbols - experimental data from Vanderover and Oehlschlaeger [46], Pitz e*t al.* [34], Vasu e*t al.* [40]; Lines - ignition delays computed using the present reaction scheme: Solid lines - lower pressure, Dashed lines - higher pressure.

hydroperoxy radicals, these result in excellent agreement with the experimentally measured slope and magnitude of ignition delays in the NTC regime of ignition as well as at low temperatures, as can be seen from Fig. 6(b) at $P = 45$ atm and Fig. 6(a) respectively. In all, a very good agreement is obtained for ignition delay times between the present scheme and the experimental data in Fig. 6 for low through high temperatures as a result of the changes introduced above.

Results for OH *time-histories:* Vasu *et al.* [41] measured OH profiles during oxidation of methylcyclohexane, with $X_{MCH} = 1000$ ppm, $X_{O_2} = 0.021$, balance Ar, at an equivalence ratio of $\phi = 0.5$ and a pressure of $P = 15\,\text{atm}$. The OH profiles predicted using the present reaction scheme are compared with the experimentally measured profiles of Vasu *et al.* in Fig. 7(a). The agreement of the peak OH value, and the time of OH rise has improved significantly compared to the combined model predictions shown in Fig. 5(b), primarily due to the changes associated with bi-radicals of butyl and pentyl reactions introduced into the model as mentioned previously. While following the experimental OH profile closely at higher temperatures, $T \sim 1280\,\text{K}$, the present model predicts delayed OH rise compared to the experiments in Fig. 7(a) at $1213\,\text{K}$.

Ignition delays were also measured by Vasu *et al.* [41] at the same conditions at which the OH

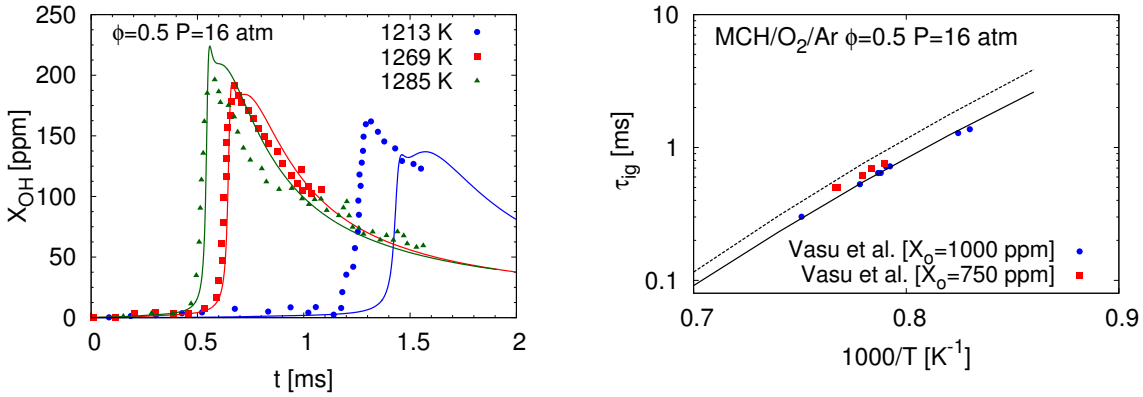

(a) OH time history (b) Ignition delay times

Figure 7: Methylcyclohexane/O_2/Ar oxidation: (a) OH profiles at $X_{MCH} = 1000$ ppm, $X_{O_2} = 0.021$, balance Ar, ($\phi = 0.5$) $P = 16$ atm (b) Ignition delay times corresponding to (i) the experimental conditions of (a), and (ii) $X_{MCH} = 750$ ppm, $\phi = 0.5$, $P = 16$ atm; Symbols - experimental data from Vasu *et al.* [41]; Solid lines - results computed using the present reaction scheme.

profiles were obtained, along with another set of ignition delay data at $X_{MCH} = 750$ ppm, $\phi = 0.5$, and $P = 15$ atm. These data are compared to the ignition delay times computed using the present chemical model in Fig. 7(b). The longer ignition delay predictions compared to the experimental data for $X_{MCH} = 750$ ppm mixtures was found to be consistent with a delayed rise in the OH time history at those conditions.

Results for laminar flame speeds: Several experimental studies have measured laminar flame speeds of methylcyclohexane/air mixtures using different measurement techniques. At atmospheric pressure and an unburnt temperature of $T_u = 353$ K, Ji *et al.* [38] determined flame speeds in a counterflow configuration. Wu *et al.* [39] measured propagation speeds of spherically expanding methylcyclohexane/air flames at atmospheric and elevated pressures with $T_u = 353$ K. Similar techniques were used by Singh *et al.* [37] to measure flame speeds at $P = 1$ atm and $T_u = 400$ K. Also, Kumar and Sung [36] used a counterflow twin-flame technique to determine flame speeds of methylcyclohexane/air mixtures at the same conditions.

The flame speeds computed using the present reaction scheme are compared with these experimental data in Fig. 8. Considering flame speeds at atmospheric pressures shown in Fig. 8(a), at $T_u = 400$ K, the model predictions are within the variability of the available experimental measurements. At $T_u = 353$ K, the computed flame speeds agree closely with at least one set of measurements for all mixture ratios, except an over-prediction at near stoichiometric conditions. At elevated pressures in Fig. 8(b), the degree of agreement with the Wu *et al.* data improves at all mixture ratios compared to that at atmospheric pressure. Also, the computed flame speeds lie within the experimental uncertainties at these higher pressures. In all, the ability of the reaction model to predict laminar flame speeds is favorable.

Methylcyclohexane summary:

It can be concluded that the present methylcyclohexane oxidation model is able to reproduce experimental ignition delay times, OH profiles, and laminar flame speeds satisfactorily. Few other

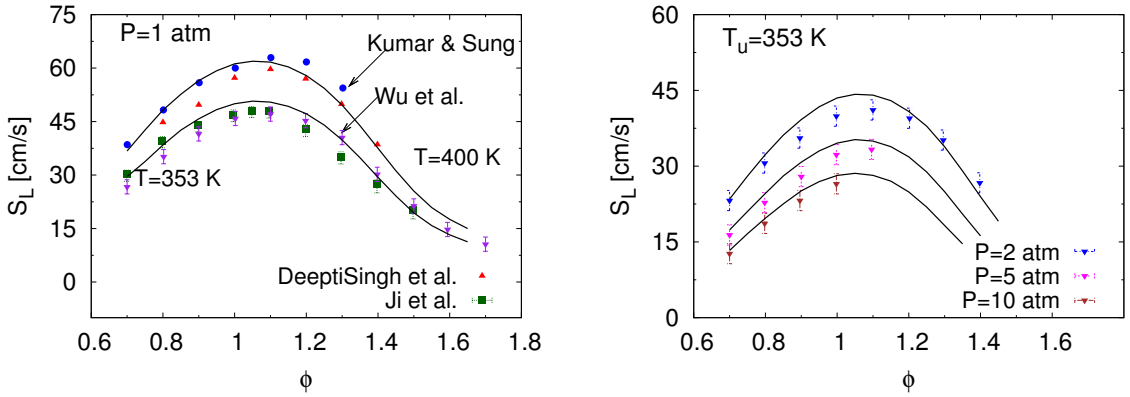

(a) $P = 1\,\text{atm}$, $T_u = 400\,\text{K}$ (b) $P = 2, 5, 10\,\text{atm}$, $T_u = 353\,\text{K}$

Figure 8: Laminar flame propagation speeds in methylcyclohexane/air mixtures: Symbols - experimental data from Kumar and Sung [36], Singh e*t al.* [37], Ji e*t al.* [38], Wu e*t al.* [39]; Solid lines - flame speeds computed using the present reaction scheme.

validation tests have also been considered (not shown here) such as species time histories in shock-tubes [35], and species concentrations in plug flow reactors [47]. The model predictions for these configurations remain favorable as well.

3.2.4 Validation of individual components in the full surrogate mechanism

With the addition of the reaction pathways of methylcyclohexane, several aromatics (especially *m*-xylene), and *n*-dodecane to the base model that already includes iso-octane, the combined chemical mechanism can be used to describe the oxidation of the jet fuel surrogate and the F-T surrogate comprised of these components, as proposed in Tables 2 and 3. The final step of this process ensures that the full surrogate kinetic model still predicts accurately each individual component. This additional step is used to evaluate any non-linear changes that might have occurred because of the added reaction modules. The results for the different test cases for the individual surrogate components were recomputed using this reaction scheme, and little changes were observed from the previous results (not shown here).

4 Performance of the proposed surrogates

4.1 Jet fuel surrogate

The capabilities of the JP-8 surrogate proposed in Table 2 are now evaluated. Global kinetic targets such as ignition delay times and laminar flame speeds computed using the present reaction scheme are compared with experimental data for a reference JP-8 fuel in this section.

Results for ignition delays

Figure 9 shows a comparison of ignition delays predicted using the present scheme with experimental measurements from Vasu *et al.* [48]. The experiments were conducted in a shock tube at

$P = 20$ atm, using fuel/air mixture ratios of $\phi = 0.5$ and 1.0. Agreement of the model and the experiments is good at high temperatures for both of the equivalence ratios that are considered here, except for a few points at $T \sim 1200$ K at $\phi = 1.0$.

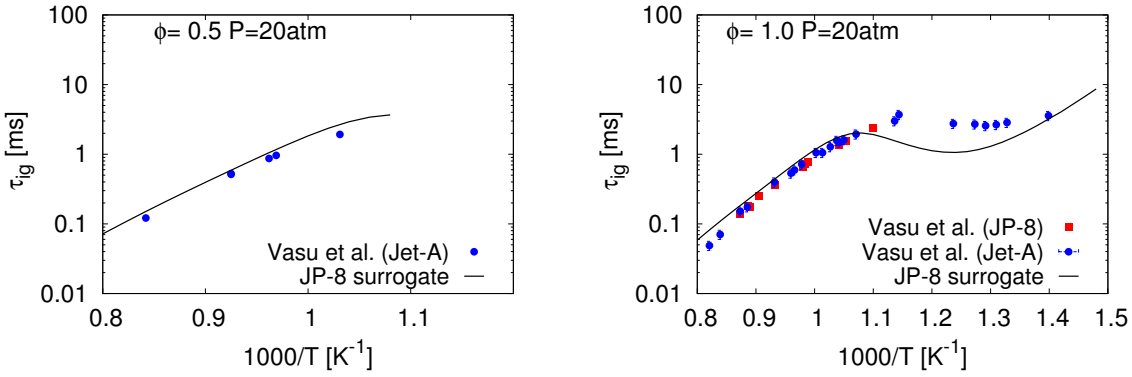

(a) $\phi = 0.5$ $P = 20$ atm (b) $\phi = 1.0$ $P = 20$ atm

Figure 9: Ignition delay times of JP-8/Jet-A fuels: Symbols - experimental data from Vasu e*t al.* [48]; Solid lines - predictions using the present reaction scheme with the JP-8 surrogate proposed in Table 2 as the fuel.

However, the present reaction scheme with the proposed JP-8 surrogate predicts shorter ignition delays than the experimental data in the NTC ignition regime. Note that *cetane number* was not considered as a target when defining the surrogate in Table 2. The cetane number of the proposed surrogate is 58.6, as opposed to the average JP-8 fuel cetane number of ~ 42. Cetane number is experimentally determined by measuring the ignition delays of the fuel under consideration in a special diesel engine called a Cooperative Fuel Research (CFR) engine, and finding that mixture of iso-cetane and *n*-cetane which results in the same ignition delay. In this way, since the operating conditions under which cetane number is measured is that of a diesel engine, the cetane number is indicative of the ignition delays in the NTC regime of ignition. Higher cetane number corresponds to faster ignition, which is consistent with the shorter ignition delays predicted by the model in the NTC region. Therefore if the cetane number of the average jet fuel is set as a constraint in the surrogate definition, then the ignition delays in the NTC region are expected to be longer and in better agreement with the experimental measurements.

A JP-8 surrogate is defined with the same components as that in the surrogate proposed in Table 2, with the requirement that the cetane number of the surrogate mixture takes a value of 42 as an additional constraint to the optimization problem. The surrogate composition that corresponds to this *lower cetane number surrogate* is provided in Table 5. The ignition delays computed using this surrogate agree better with the ignition delay measurements in the NTC regime, with little effect in the degree of agreement at high temperatures, as shown in Fig. 10.

Considering the composition of this lower cetane surrogate, the aromatic (*m*-xylene) portion remains similar to the previous surrogate due to the threshold sooting index constraint. However, it can be observed that the amount of paraffins and naphthenes, as well as the molecular weight of the surrogate mixture could no more be reproduced in this definition of the surrogate. Since

Target properties	Jet-A/JP-8 properties	Surrogate Definition	
		JP-8 Surrogate	Lower Cetane Surrogate
H/C ratio	1.91 ± 0.05	1.94	1.89
Average formula	$C_{11}H_{21}$	$C_{9.64}H_{18.75}$	$C_{8.47}H_{16.03}$
Liquid density (kg/l)	0.810	0.769	0.776
Molecular weight (g/mol)	153	134.80	117.94
TSI	15	15.34	15.00
Cetane Number	42	58.6	42
Composition (% volume)	$\sim 60\%$ paraffins $\sim 20\%$ cyclo paraffins $\sim 18\%$ aromatics	62% *n*-dodecane 19.8% methylcyclohexane 17.6% *m*-xylene	37.2% *n*-dodecane 43.8% methylcyclohexane 18.9% *m*-xylene

Table 5: Jet fuel surrogate

n-dodecane has the shortest ignition delays in the NTC region among the components of the surrogate mixture (with a corresponding high cetane number of 85), while methylcyclohexane has a low cetane number of 20, the contribution from *n*-dodecane in the surrogate mixture is reduced and that of methylcyclohexane increased, in order to achieve the mixture cetane number of 42. Including additional components such as a branched alkane (which has a lower cetane number) in the surrogate mixture would help to reduce the overall cetane number of the mixture. In addition, selecting a heavier aromatic or naphthene could improve the carbon number of the surrogate mixture, and help achieve the desired target properties, as well as predict ignition delays in closer agreement with experiments.

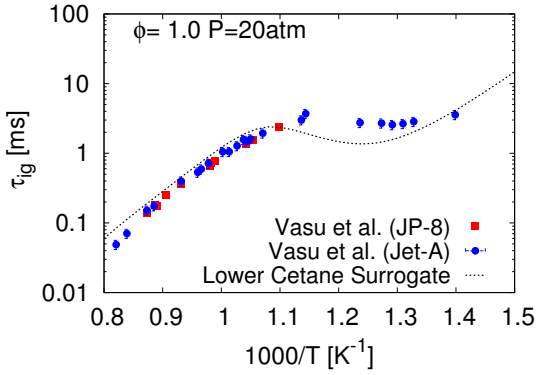

Figure 10: Ignition delay times of JP-8/Jet-A fuels: Symbols - experimental data from Vasu e*t al.* [48]; Dotted lines - predictions using the present reaction scheme with the *lower cetane number surrogate* for JP-8 fuel whose composition is listed in Table 5.

Results for laminar flame speeds

Ji *et al.* [49] measured laminar flame speeds of JP-7 and JP-8 fuels at atmospheric pressure and at an unburnt temperature of $T_u = 403\,\mathrm{K}$. The flame speeds computed using the present reaction scheme with the previously proposed jet surrogate as the fuel (from Table 2) are compared with these experimental data in Fig. 11(a). The flame speed predictions closely follow the JP-8 flame

speeds at all fuel/air ratios. It can be seen that the experimentally determined flame speeds of *n*-dodecane are approximately equal to those of the JP-8 fuel, justifying the use of this component as the significant alkane within the surrogate. However, the flame speeds of methylcyclohexane are only shorter by 2–5 cm/s at different equivalence ratios, and interestingly, as a result, the *lower cetane number surrogate* proposed in Table 5 also resulted in similar flame speeds as shown in Fig. 11(a), although a little shorter (< 3 cm/s) at lean fuel/air ratios.

With this discussion, the ability of the present scheme to predict global oxidation characteristics of real JP-8 fuels, such as ignition delays at high temperatures and laminar flame speeds, can be concluded to be good. The chemical model will be further assessed in other configurations of interest in future.

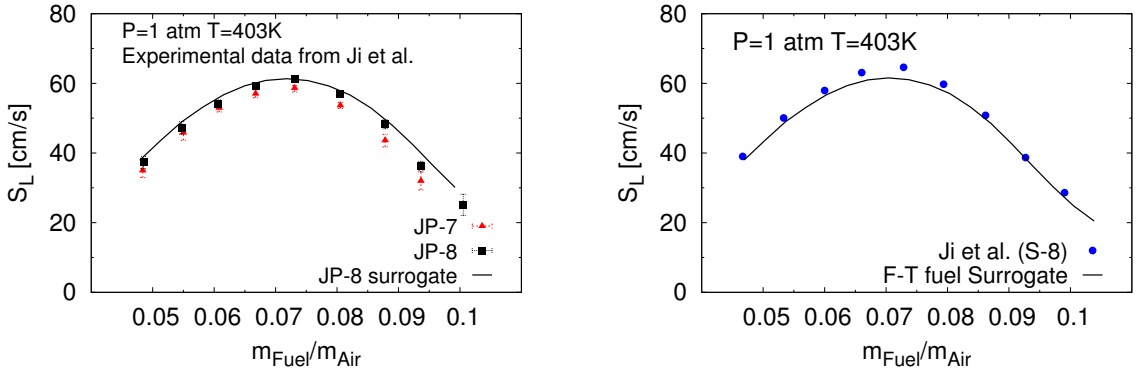

Figure 11: Laminar flame speeds of jet fuel and F-T fuels: (a) Symbols - experimental data for jet fuels from Ji e*t al.* [49]; Solid lines - flame speed predictions using the present reaction scheme with the Jet fuel surrogate proposed in Table 2 as the fuel (b) Symbols - experimental data from Ji e*t al.* [50]; Solid lines - flame speed predictions using the present reaction scheme with the F-T surrogate proposed in Table 3 as the fuel.

4.2 Fischer-Tropsch fuel surrogate

The performance of the F-T surrogate proposed in Table 3 is now discussed. Laminar flame speeds computed using the present reaction scheme are compared with experimental data for a real F-T fuel here. Ji *et al.* [50] measured flame speeds of a synthetic S-8 fuel, obtained by Fischer-Tropsch process at unburnt temperature of $T_u = 403$ K, $P = 1$ atm. Figure 11(b) shows the predictions of the present reaction scheme using the F-T surrogate proposed in Table 3 as the fuel, in comparison to the experimental flame speeds. The predictions are in close agreement with the experimental data at most of the fuel/air ratios, while they under-predict the flame speeds at few points. The ability of the chemical model to describe F-T fuels will be assessed in more detail when more experimental data becomes available for other test configurations of interest, such as ignition delays and flow reactor measurements.

5 Conclusions

In using surrogate fuels in place of real fuels, the two main challenges of (i) surrogate definition and (ii) design of a compact and reliable chemical model for the surrogate have been addressed in this work in a systematic manner. The ideas presented here could be extended to any real fuel, with appropriate choice of surrogate fuel components and target real fuel properties to be considered to define the surrogate.

The components included in the surrogate are selected by identifying a representative compound for each of the major hydrocarbon classes found in the real fuel. A *constrained optimization* approach is proposed to determine the surrogate composition and surrogates are proposed for jet fuels (JP-8/Jet-A) and Fischer-Tropsch fuels. The surrogate mixtures are composed of *n*-dodecane (to represent normal alkanes), iso-octane (to represent branched alkanes), methylcyclohexane (to represent cyclic alkanes), and *m*-xylene (to represent aromatics).

Following this, a *component library* approach has been discussed to develop a chemical kinetic model for the proposed surrogates. This essentially describes a consistent and simplified framework for the assembly of a compact reaction mechanism for surrogates. This approach has been demonstrated in the present work, in the context of jet fuel (JP-8/Jet-A) and Fischer-Tropsch fuel surrogates. In the process, the present work involved development of a chemical kinetic model to describe the low through high temperature oxidation of methylcyclohexane, following the chemical model development for the other surrogate fuel components in our previous works [27, 28, 31]. In order to better describe the kinetics of methylcyclohexane oxidation, a few changes have been introduced in the combined mechanism based on rate recommendations from theoretical and experimental work available in the literature. The revised model has been comprehensively validated against a range of experimental data sets at low through high temperatures, and the model predictions have been found to be satisfactory for the test configurations considered here.

Thereafter, the model predictions using the proposed surrogates as fuels are compared against ignition delay and flame speed measurements for representative JP-8 fuels and Fischer-Tropsch fuels. The real fuel flame speeds were found to be predicted well by the reaction scheme for the proposed surrogates. The computed ignition delays for the JP-8 surrogate at different equivalence ratios and at high temperatures were in good agreement with experimental data for the jet fuels. Some differences were observed when comparing the model predictions for the proposed JP-8 surrogate with ignition delay data at lower temperatures, $T < 1000\,\mathrm{K}$. A surrogate with a lower cetane number has been proposed, and this was found to achieve better agreement with the ignition delay data at these lower temperatures, however at the cost of the jet fuel surrogate being unable to reproduce the amount of the different hydrocarbons classes of the real fuel. This suggests to re-consider the fuel components chosen to be included in the JP-8 surrogate mixture in order for better ignition delay predictions at lower temperatures as well. However, for most high temperature applications in which low temperature chemistry might not be required to be represented accurately, the high cetane number JP-8 surrogate proposed in Table 2 remains valid and appropriate.

Acknowledgements

The authors greatly acknowledge funding by the Air Force Office of Scientific Research and NASA.

References

[1] W. J. Pitz, N. P. Cernansky, F. L. Dryer, F. N. Egolfopoulos, J. T. Farrell, D. G. Friend, and H. Pitsch. *SAE Paper No. 2007-01-0175*, (2007) .

[2] J. T. Farrell, N. P. Cernansky, F. L. Dryer, D. G. Friend, C. A. Hergart, C. K. Law, R. M. McDavid, C. J. Mueller, A. K. Patel, and H. Pitsch. *SAE Paper No. 2007-01-0201*, (2007) .

[3] M. Colket, T. Edwards, S. Williams, N. P. Cernansky, D. L. Miller, F. Egolfopoulos, P. Lindstedt, K. Seshadri, F. L. Dryer, C. K. Law, D. Friend, D. B. Lenhert, H. Pitsch, A. F. Sarofim, M. Smooke, and W. Tsang. *AIAA 2007-770*, (2007) .

[4] T. Edwards and L. Q. Maurice. *J. Prop. Power*, 17 (2001) 461–466.

[5] E. Ranzi, A. Frassoldati, S. Granata, and T. Faravelli. *Int. Eng. Chem. Res.*, 44 (2005) 5170–5183.

[6] A. Violi, S Yan, E. G. Eddings, A. F. Sarofim, S. Granata, T. Faravelli, and E. Ranzi. *Combustion Science and Technology*, 174 (2002) 399–417.

[7] S. Dooley, S. H. Won, M. Chaos, J. Heyne, Y. Ju, F. L. Dryer, K. Kumar, C.-J Sung, H. Wang, M. A. Oehlschlaeger, R. J. Santoro, and T. A. Litzinger. *Combust. Flame*, 157 (2010) 2333 – 2339.

[8] S. Humer, A. Frassoldati, S. Granata, T. Faravelli, E. Ranzi, R. Seiser, and K. Seshadri. *Proceedings of the Combustion Institute*, 31 (2007) 393 – 400.

[9] A. J. Dean, O. G. Penyazkov, K. L. Sevruk, and B. Varatharajan. *Proceedings of the Combustion Institute*, 31 (2007) 2481–2488.

[10] C. V. Naik, K. V. Puduppakkam, A. Modak, E. Meeks, Y. L. Wang, Q. Feng, and T. T. Tsotsis. *Combust. Flame*, 158 (2011) 434 – 445.

[11] I. P. Androulakis, M. D. Weisel, C. S. Hsu, K. Qian, L. A. Green, J. T. Farrell, and K. Nakakita. *Energy & Fuels*, 19 (2005) 111–119.

[12] H. Wang, E. Dames, B. Sirjean, D. A. Sheen, R. Tangko, A. Violi, J. Y. W. Lai, F. N. Egolfopoulos, D. F. Davidson, R. K. Hanson, C. T. Bowman, C. K. Law, W. Tsang, N. P. Cernansky, D. L. Miller, and R. P. Lindstedt. *jetSurF 2.0 (http://melchior.usc.edu/JetSurF/JetSurF2.0)* .

[13] S. Honnet, K. Seshadri, U. Niemann, and N. Peters. *Proceedings of the Combustion Institute*, 32 (2009) 485 – 492.

[14] A. Agosta, N. P. Cernansky, D. L. Miller, T. Faravelli, and E. Ranzi. *Experimental Thermal and Fluid Science*, 28 (2004) 701 – 708.

[15] K. E. Niemeyer, C.-J Sung, and M. P. Raju. *Combust. Flame*, 157 (2010) 1760 – 1770.

[16] S. S. Vasu, D. F. Davidson, Z. Hong, V. Vasudevan, and R. K. Hanson. *Proc. Combust. Inst.*, 32 (1) (2009) 173–180.

[17] *Technical Report, Chevron Corporation*, (2004) .

[18] J. Bacha, J. Freel, A. Gibbs, L. Gibbs, G. Hemigaus, N. Hogue, D. Lesnini, J. Lind, J. Maybury, and J. Morris. *Technical Report, Chevron Corporation*, (2005) .

[19] J. Bacha, J. Freel, A. Gibbs, L. Gibbs, G. Hemigaus, K. Hoekman, J. Horn, M. Ingham, L. Jossens, D. Kohler, D. Lesnini, J. McGeehan, N. Nikanjam, E. Olsen, R. Organ, B. Scott, M. Sztenderowicz, A. Tiedemann, C. Walker, J. Lind, J. Jones, D. Scott, and J. Mills. *Technical Report, Chevron Corporation*, (2007) .

[20] H.F. Calcote and D.M. Manos. *Combust. Flame*, 49 (1983) 289–304.

[21] Y. Yang, A. L. Boehman, and R. J. Santoro. *Combust. Flame*, 149 (2007) 191–205.

[22] S. Yan, E. G. Eddings, A. B. Palotas, R. J. Pugmire, and A. F. Sarofim. *Energy & Fuels*, 19 (2005) 2408–2415.

[23] S. W. Benson. *Thermochemical Kinetics : Methods for the Estimation of Thermo- chemical Data and Rate Parameters*. Wiley, New York, 1976.

[24] P. Pepiot-Desjardins. *PhD. thesis, Department of Mechanical Engineering, Stanford University*. 2008.

[25] P. Pepiot-Desjardins and H. Pitsch. *Combust. Flame*, 154 (2008) 67–81.

[26] P. Pepiot-Desjardins and H. Pitsch. *Combust. Theory. Mod.*, 12 (6) (2008) 1089–1108.

[27] G. Blanquart, P. Pepiot-Desjardins, and H. Pitsch. *Combust. Flame*, 156 (2009) 588–607.

[28] K. Narayanaswamy, G. Blanquart, and H. Pitsch. *Combust. Flame*, 157 (10) (2010) 1879–1898.

[29] S. M. Sarathy, C. K. Westbrook, M. Mehl, W. J. Pitz, C. Togbe, P. Dagaut, H. Wang, M. A. Oehlschlaeger, U. Niemann, and K. Seshadri. *Combust. Flame*, 158 (2011) 2338–2357.

[30] Z. Hong, D. F. Davidson, and R. K. Hanson. *Combust. Flame*, 158 (2011) 633–644.

[31] K. Narayanaswamy, P. Pepiot, and H. Pitsch. *Manuscript in preparation*, (2013) .

[32] S. Granata, T. Faravelli, and E. Ranzi. *Combust. Flame.*, 132 (2003) 533–544.

[33] J. P. Orme, H. J. Curran, and J. M. Simmie. *J. Phys. Chem. A.*, 110 (2006) 114–131.

[34] W. J. Pitz, C. V. Naik, T. N. Mhaolduin, C. K. Westbrook, H. J. Curran, J. P. Orme, and J. M. Simmie. *Proc. Combust. Inst.*, 31 (1) (2007) 267–275.

[35] Z. Hong, D. F. Davidson, and R. K. Hanson. *Combust. Flame*, 158 (2011) 633–644.

[36] K. Kumar and C.J. Sung. *Energy & Fuels*, 24 (2010) 3840–3849.

[37] D. Singh, T. Nishiie, and L. Qiao. *Central States Technical Meeting*, (2010) .

[38] C. Ji, E. Dames, B. Sirjean, H. Wang, and F. N. Egolfopoulos. *Proc. Combust. Inst.*, 33 (2011) 971–978.

[39] F. Wu, A. P. Kelley, and C. K. Law. *Combust. Flame.*, 159 (4) (2012) 1417–1425.

[40] S. S. Vasu, D. F. Davidson, Z. Hong, V. Vasudevan, and R. K. Hanson. *Energy & Fuels*, 23 (2009) 175–185.

[41] S. S. Vasu, D. F. Davidson, and R. K. Hanson. *Combust. Flame*, 156 (2009) 736–749.

[42] E. J. Silke, W. J. Pitz, C. K. Westbrook, and M. Ribaucour. *J. Phys. Chem. A.*, 111 (2007) 3761–3775.

[43] B. Sirjean, P. A. Glaude, M. F. Ruiz-Lopez, and R. Fournet. *J. Phys. Chem. A.*, 112 (2008) 11598–11610.

[44] B. Sirjean, P. A. Glaude, M. F. Ruiz-Lopez, and R. Fournet. *J. Phys. Chem. A.*, 113 (2009) 6924–6935.

[45] H. Pitsch and M. Bollig. *Institut fur Technische Mechanik, RWTH Aachen*, (1993) journal.

[46] J. Vanderover and M. A. Oehlschlaeger. *Int. J. Chem. Kinet.*, 41 (2009) 82–91.

[47] S. Zeppieri, K. Brezinsky, and I. Glassman. *Combust. Flame*, 108 (2009) 266–286.

[48] S.S. Vasu, D.F. Davidson, and R.K. Hanson. *Combust. Flame*, 152 (2008) 125–143.

[49] C. Ji, X. You, A. T. Holley, Y. L. Wang, F. N. Egolfopoulos, and H. Wang. *46th AIAA Aerospace Sciences Meeting and Exhibit, Reno, Nevada*, 7 (2008) .

[50] C. Ji, Y.L. Wang, and F.N. Egolfopoulos. *Journal of Propulsion and Power*, 27 (2011) 856.